DEUTSCHES ELEKTRONEN-SYNCHROTRON DESY

DESY 82-018
March 1982

MEASUREMENT OF INCLUSIVE γ AND π^0 SPECTRA AND A COMPARISON OF THE NEUTRAL AND CHARGED COMPONENTS IN HADRONIC EVENTS IN e^+e^- ANNIHILATION AT 34 GeV

by

CELLO Collaboration

NOTKESTRASSE 85 · 2 HAMBURG 52

To be sure that your preprints are promptly included in the
HIGH ENERGY PHYSICS INDEX ,
send them to the following address (if possible by air mail) :

DESY
Bibliothek
Notkestrasse 85
2 Hamburg 52
Germany

DESY 82-018
March 1982

Measurement of Inclusive γ and π^0 Spectra and a Comparison of the Neutral and Charged Components in Hadronic Events in e^+e^- Annihilation at 34 GeV

CELLO Collaboration

H.J. Behrend, Ch. Chen[1], H. Fenner, J.H. Field[2], V. Schröder, H. Sindt
Deutsches Elektronen Synchrotron DESY, Hamburg, Germany

G. D'Agostini, W.-D. Apel, S. Banerjee, J. Bodenkamp, D. Chrobaczek, J. Engler, G. Flügge, D.C. Fries, W. Fues, K. Gamerdinger, G. Hopp, H. Küster, H. Müller, H. Randoll, G. Schmidt, H. Schneider
Kernforschungszentrum Karlsruhe and Universität Karlsruhe, Karlsruhe, Germany

W. de Boer, G. Buschhorn, G. Grindhammer, P. Grosse-Wiesmann, B. Gunderson, C. Kiesling, R. Kotthaus, U. Kruse[3], H. Lierl, D. Lüers, T. Meyer[4], H. Oberlack, P. Schacht, M.J. Schachter[5], A. Snyder[6], H. Steiner[7]
Max-Planck-Institut für Physik und Astrophysik, München, Germany

G. Carnesecchi, P. Colas, A. Cordier, M. Davier, D. Fournier, J.F. Grivaz, J. Haissinski, V. Journe, A. Klarsfeld, F. Laplanche, F. Le Diberder, U. Mallik, J.J. Veillet
Laboratoire de l'Accélérateur Linéaire, Orsay, France

R. George, M. Goldberg, B. Grossetete, O. Hamon, F. Kapusta, F. Kovacs, G. London[8], L. Poggioli, M. Rivoal
Laboratoire de la Physique Nucléaire et Hautes Energies, University of Paris, Paris, France

R. Aleksan, J. Bouchez, G. Cozzika, Y. Ducros, A. Gaidot, S. Jadach[9], Y. Lavagne, J. Pamela, J.P. Pansart, F. Pierre
Centre d'Etudes Nucléaires, Saclay, France

---

1) Visitor from the Institute of High Energy Physics, Chinese Academy of Science, Peking, People's Republic of China

2) On leave of absence, presently at University of Paris

3) Visitor from the University of Illinois, Urbana, USA

4) Now at the University of Wisconsin, Madison, USA

5) Now at DESY, Hamburg, Germany

6) Now at Rutgers University, New Brunswick, USA

7) Alexander von Humboldt Foundation, Senior American Scientist, University of California, Berkeley, USA

8) On leave of absence, presently at University of California, Berkeley, USA

9) Visitor from the University of Cracow, Poland

Abstract

The photonic part of multihadronic e^+e^- annihilation events has been analyzed at a c.m. energy of 34 GeV. The photonic energy fraction per event is determined to be $f_\gamma = 0.251 \pm 0.003$ (stat.) $\pm$ 0.04 (syst.). The neutral and charged components of the events are analyzed separately revealing close similarity in thrust axis directions and momentum distributions in agreement with the hypothesis that most photons result from π^0 decay. π^0's are reconstructed separately and used to determine the inclusive cross section.Comparing these cross sections with lower energy data from SPEAR we find some indication for scaling violation.

1. Introduction

Most of our knowledge about e^+e^- annihilation into multihadronic final states at PETRA energies comes from the study of charged particles. In this paper we present results on global topological quantities based on an analysis of individual photons, and on a comparison between the photonic and charged components. We determine the inclusive production cross section of photons and π^0's.

The data were taken with the CELLO [1] detector at PETRA at an average center of mass (c.m.) energy of 34 GeV. The data sample of 2441 events corresponds to an integrated luminosity of 7.87 pb^{-1}. The trigger for the multihadronic final states and the event selection criteria have been described previously [2]. The neutral particle analysis uses the barrel liquid argon calorimeter which has a solid angle acceptance of 86% of 4 π. Each of 16 calorimeter modules samples the energy deposited by particles up to 17 times in depth leading to spatial measurements in 6 layers up to a maximum depth of 20 radiation length (X_o). Each layer consists of channels in three orientations [1] . We obtain an energy resolution of $\sigma(E)/E = 13\%/\sqrt{E}$ (GeV) and an angular resolution of 4 mrad. The jet-structure of the multihadronic final states causes a substantial overlap between clusters of deposited charge from different photons, and from photons and charged tracks. Therefore the actual resolution obtained in a multihadron event depends on the γ-energy and event topology and can vary by up to a factor of 2.

2. Analysis Method

The data were processed through the reconstruction programs for charged tracks in the inner detector and for showers in the barrel liquid argon calorimeter ($|\cos\theta| < 0.86$).

In the shower reconstruction program clusters in each of the six layers of the modules are reconstructed using the geometrical correlations between the three channel orientations and between neighbouring channels in depth. Two-dimensional clusters are formed and then linked to give three-dimensional showers. The topology determination - single or several overlapping photons - is done by scanning the two-dimensional clusters for structures in the pulse height distribution and checking their spatial distribution. Monte-Carlo (MC) studies show that the efficiency and resolution for two photons

separated by an angle larger than 130 mrad are similar to those for single photons. At an angle of 65 mrad the efficiency for separating two photons is still about 50%. The energy and angular resolutions are, in this case, worse by up to a factor of two depending on the photon energies considered.

Charged tracks as found in the inner detector are extrapolated into the liquid argon calorimeter and the extrapolated track position is used in the two-dimensional cluster reconstruction. Thus the final showers are separated into "charged showers" (showers which are found to be linked to charged tracks) and "neutral showers" (showers for which no link is found to charged tracks). The efficiency of this linking procedure for tracks with momenta above 1 GeV was found to be 74% in multihadronic events. The longitudinal development of the neutral showers is then used to distinguish photons from K^o's, neutrons or charged particles where the link failed. For the selection of well measured photons the following criteria are used:

- Photons that result from three or more overlapping showers are rejected.
- Neutral showers are only accepted if more than 20% of the total charge is deposited in the second and third layer of the liquid argon calorimeter extending from 3 to 8 X_o.
- Showers corresponding to an energy of less than 3 GeV are only accepted if no charge is found in the sixth layer (> 16 X_o).

A lower limit for the photon energy E_γ = 100 MeV is imposed by the shower reconstruction program. These cuts were checked using the test data of the liquid argon calorimeter prototype module [3], Bhabha events and QED two photon events ($e^+e^- \to e^+e^-e^+e^-$). The resulting efficiency due to these cuts for reconstructed photons is 0.91. The background due to misidentified n or K_L^o or charged particles where the link failed is less than 3.5%.

Corrections for acceptance, reconstruction inefficiencies, losses due to the cuts described above and for radiative effects were determined by MC methods. Multihadron events were generated assuming $q\bar{q}$ and $q\bar{q}g$ production according to first order QCD [4] (q = u,d,s,c,b and α_s = 0.19) with subsequent fragmentation [5] (σ_q = 0.30 GeV/c). These events were passed through a detailed detector simulation using the EGS and HETC codes [6] for the simulation of charge deposition in the liquid argon calorimeter and through the same reconstruction chain as the real data.

3. Inclusive γ production and photonic energy

Fig. 1 shows the resulting differential cross section for inclusive photon production. The error bars indicate the statistical errors only. An overall systematic error of 14% due to uncertainties in the overall normalization, calibration and MC correction has to be added. The average multiplicity of photons with an energy above 100 MeV is found to be 15.8 ± 1.0.

Next we determine the fraction f_γ of the total c.m. energy carried by photons. In order to minimize edge effects we selected events with a cut of $|\cos\theta| < 0.82$ on the angle of the thrust axis with the beam direction. In addition we requested more than 6% detected photonic energy in the event. The observed energy fraction was corrected for radiative effects in the detector, for misidentified or lost photons and for acceptance cuts, yielding an average correction factor of 1.30. This correction includes the geometrical acceptance correction of 1.53 (including events with initial state radiation), the correction due to the cuts applied for the photon selection of 1.09, the correction due to the conversion of photons in the beam pipe or the inner detector of 1.03 and the correction for initial state radiation of 0.76. The distribution of the corrected photonic energy fraction per event is shown in fig.2. The average is found to be 0.268 ± 0.003. It includes photons resultung from π^0's from K^0_S decays. From MC calculations [4,5] we estimate this contribution to f_γ to be 0.017 ± 0.005, in agreement with a recent comparison with measurements [7]. Thus we finally get for the photonic energy fraction

$$f_\gamma = 0.251 \pm 0.003 \text{ (stat.)} \pm 0.04 \text{ (syst.)} \qquad (1)$$

The systematic error is mostly determined by uncertainties in the MC simulation.

As an independent check we have analyzed the same data using a calorimetric method without photon reconstruction. Details of the method are described elsewhere [8]. We found $f_\gamma = 0.260 \pm 0.004$ (stat.) ± 0.04 (syst.) in agreement with (1). The systematic uncertainties attached to the two methods are of widely different origin. The average of the two methods yields $f_\gamma = 0.255 \pm 0.04$. This measurement is in agreement with a recent measurement of 0.30 ± 0.03 at a c.m. energy of 34.9 GeV by the JADE collaboration [7].

4. Comparison of the Photonic and Charged Components

The topological characteristics of the neutral and charged components in the multihadronic events were analyzed using thrust and sphericity as variables. A comparison of the thrust distributions for the charged and the neutral component is given in Fig. 3. The distributions are fully corrected. They are similar although the thrust distribution for photons peaks at a lower value and is somewhat broader than the corresponding distribution for charged particles. These effects are reproduced in the MC generated events and are mostly due to the decay of π^0 and η into photons.

Fig. 4 shows the MC-corrected distribution of the cosine of the angle α between the thrust axes determined independently from the neutral and the charged components alone. The peaking at small angles indicates that the neutral energy follows the charged energy closely. Large angular deviations were found to originate essentially from events where one of the jets is almost completely neutral or charged. It is therefore reasonable to form a common thrust axis for an event using both charged particles and photons.

In figs. 5 and 6 we compare the MC corrected longitudinal (P_L) and transverse (P_T) momentum distributions of the photons and charged particles relative to the common thrust axis determined from both the neutral and the charged components. The photons have roughly half the momentum of the charged particles. This indicates that most of them result from the decay of π^0, if we assume the inclusive π^0 production to be similar to the inclusive charged π production. In Table 1 the MC corrected mean values of some topological quantities for the charged particles and photons are summarized.

5. Inclusive π^0 Production

From the measured photons we reconstructed π^0's with momenta between 0.9 and 8 GeV/c. To supress the background further and to select well measured photons the following more stringent cuts have been applied in addition to the cuts described above:

- Photons whose showers overlap clusters linked to charged tracks are rejected.
- Two photons with overlapping showers are kept only if the double structure found in the reconstruction program is present in the second and third layer. These are the layers that have a fine lateral sampling.
- Photons whose showers do not extend in depth over at least three layers are rejected.

- The minimum photon energy is 300 MeV.

After all these cuts, 12.4% of all photons were left, the most severe cut being the photon energy cut. Fig. 7 shows the distribution of the invariant mass combinations $m_{\gamma\gamma}$ of all remaining γ-pairs. A clear π^0 peak is seen. A fit to the data using a gaussian plus a background term given by a second order polynomial yields a width of the π^0-peak of $\sigma = 23 \pm 5$ MeV/c^2.

For the further analysis of the inclusive π^0 cross section, two different methods were applied. In the first method the χ^2 corresponding to the π^0 hypothesis were calculated for all two photon combinations. First the two photons with the lowest χ^2 were selected, then from the remaining photons the two with the lowest χ^2 were found. This procedure has been repeated until χ^2 was unacceptably large. For the selected photons, a regrouping into all possible pair combinations was tried through all permutations and the permutation yielding the lowest overall χ^2 was kept. Finally a π^0 candidate was kept only if $m_{\gamma\gamma}$ was in the range $60 < m_{\gamma\gamma} < 210$ MeV/c^2. Depending on the π^0-momentum, this yields an overall acceptance of 5% to 8%.

This selection method has been tested using MC generated events, that have been passed through the same analysis chain as the real events. For π^0 momenta above 1.2 GeV/c the background contamination is on the average 14%. For momenta below 1.2 GeV/c the background is substantially larger (37%). Fig.8 shows the distribution of the invariant mass combinations of photon pairs which are assigned to π^0's selected by the method described above and all the mass combinations of the unassigned photons.

In the second method, the π^0 cross section has been obtained using a simple background subtraction. All possible combinations of γ-pairs were binned according to the momentum of the pair. For each momentum bin the background was estimated by forming pairs with γ's coming from different events. The correlation of the gammas due to the jet structure was taken into account by rotating each event so that the sphericity axes coincide. The background for each π^0 momentum bin thus determined was normalized using the mass spectrum above the π^0 mass ($270 < m_{\gamma\gamma} < 450$ MeV/c^2). The π^0 mass interval was $60 < m_{\gamma\gamma} < 210$ MeV/c^2. The dotted curve in fig. 7 shows this normalized background distribution for all γ-pairs. The π^0 cross sections from the two methods were in good agreement and therefore the average of both methods was used. Figs. 9a, b show the inclusive π^0 cross section. The error bars include (added in quadrature) the statistical errors, the errors due to the background subtraction (varying from 3% to 15%), and all systematic errors due to the absolute normalization (5%), calibration (6%) and MC simulation (typically about 15%).

In Fig. 9a we compare our inclusive π^0 cross sections with those from TASSO [9] at 14 and 34 GeV and with those from SPEAR [10] at lower energies. For $x < 0.15$ our values are somewhat higher than the TASSO values at the same energy. For $x > 0.15$ we observe good agreement with TASSO both at 14 and 34 GeV. In this x-range the PETRA data at 14 and 34 GeV are lower than the corresponding data from SPEAR at $\sim$ 6 GeV, indicating some scaling violations which is expected from QCD. Better data in the high x-range are clearly important to confirm this effect.

Fig. 9b shows our π^0-values in comparison with the inclusive charged hadron cross sections determined from the same data [11]. In addition the inclusive cross section for charged π's at the same energy from TASSO [12] are shown. Although the π^0- spectrum appears to be somewhat softer than the $\pi^\pm$- spectrum, the data are in agreement for $x > 0.15$. For $x < 0.15$ the π^0- data are somewhat higher than the $\pi^\pm$- data, but not inconsistent within the large errors.

Conclusions

Comparing the photonic and charged components in multihadronic events at a c.m. energy of 34 GeV we determined the photonic energy fraction from reconstructed photons to $f_\gamma = 0.251 \pm 0.003$ (stat.) $\pm$ 0.04 (syst.). The thrust distribution as determined separately from photons and charged particles are similar. The longitudinal and transverse momentum distributions of photons and charged particles indicate that the dominant source of photons is the π^0-production. From the measurement of the inclusive π^0-cross section we found some indication of scaling violation going from SPEAR to PETRA energies.

Acknowledgement

We are indebted to the PETRA machine group and the DESY computer center for their excellent support during the experiments. We acknowledge the efforts of our engineers and technicians and in particular the support of Dr. Horlitz and G. Mayaux and their groups in the operation of the magnet system. The visiting groups wish to thank the DESY directorate for the support and kind hospitality extended to them. This work was partly supported by the Bundesministerium for Forschung und Technologie.

Table 1 Average values for sphericity (S), thrust (T), average longitudinal $\langle\langle P_L \rangle\rangle$ and average transverse momenta $\langle\langle P_T \rangle\rangle$ for photons and charged particles at E = 34 GeV.

	Photons	Charged Particles
$\langle S \rangle$	0.19 ± 0.04	0.13 ± 0.04
$\langle T \rangle$	0.86 ± 0.03	0.89 ± 0.02
$\langle\langle P_L \rangle\rangle$	0.54 ± 0.09 [GeV/c]	1.48 ± 0.11 [GeV/c]
$\langle\langle P_T \rangle\rangle$	0.22 ± 0.09 [GeV/c]	0.46 ± 0.05 [GeV/c]

REFERENCES

[1] CELLO-Coll., H.-J. Behrend et al., Phys. Scripta 23 (1981), 610

[2] CELLO-Coll., H.-J. Behrend et al., DESY 81-029 (1981), accepted for publication in Phys. Lett. B.

[3] W.D. Apel et al., to be published in Nucl. Instr. and Methods

[4] P. Hoyer et al., Nucl. Phys. B161 (1979), 349
A. Ali et al., Z. f. Physik C1 (1979), 203

[5] R.D. Field, R.P. Feynman, Phys. Rev. D15 (1977), 2590
Nucl. Phys. 138 (1978), 1

[6] R.L. Ford and W.R. Nelson, EGS code, SLAC Report Nr. 210 (1978) RSIC Computer Code Collection, HETC Code, Oak Ridge National Laboratory, CCC-178

[7] JADE-Coll., W. Bartel et al., DESY 81-025 (1981)

[8] CELLO-Coll., H.-J. Behrend et al., DESY 82-017

[9] TASSO-Coll., R. Brandelik et al., DESY 81-069 (1981), Phys. Lett. 108B (1982), 71

[10] D.L. Scharre et al., Phys. Rev. Lett. 41 (1978), 1005

[11] CELLO-Coll., H.-J. Behrend et al., to be published

[12] TASSO-Coll., R. Brandelik et al., submitted to Phys. Lett. B.

FIGURE CAPTIONS

Fig. 1 Inclusive cross section $d\sigma/dE$ for photons. The error bars indicate statistical errors only. An overall systematic error of 14% is not included.

Fig. 2 Distribution of the fraction of total c.m. energy carried by photons in an event.

Fig. 3 Distribution of the thrust of an event determined separately from charged particles (triangles) and photons (circles). The solid (dashed) lines indicate the corresponding distribution from MC data for charged particles (photons).

Fig. 4 Distribution of the angle between the thrust axes determined independently from the neutral and the charged components.

Fig. 5 Distribution of the momentum components parallel to the common thrust axis for charged particles (triangles) and photons (circles).

Fig. 6 Distribution of the momentum components transverse to the common thrust axis for charged particles (triangles) and photons (circles).

Fig. 7 Distribution of the invariant mass combinations of all photon-pairs. The fit to the data using a gaussian plus a second order polynomial background is also displayed. The dotted line represents the background as found by method II.

Fig. 8 Distribution of the invariant mass of the photon pairs after the π^0-reconstruction with method I.

Fig. 9a Inclusive cross sections $(s/\beta)\, d\sigma/dx$ for π^0 production at E_{cm} = 34 GeV. In addition π^0 inclusive data from lower energies (Ref. 10) and the same energy (Ref. 9) are shown.

Fig. 9b Comparison of the inclusive cross sections $s\, d\sigma/dx$ for π^0 production with one half of the inclusive cross section for $\pi^\pm$ (Ref. 12) and all charged particles (Ref. 11) at the same energy.

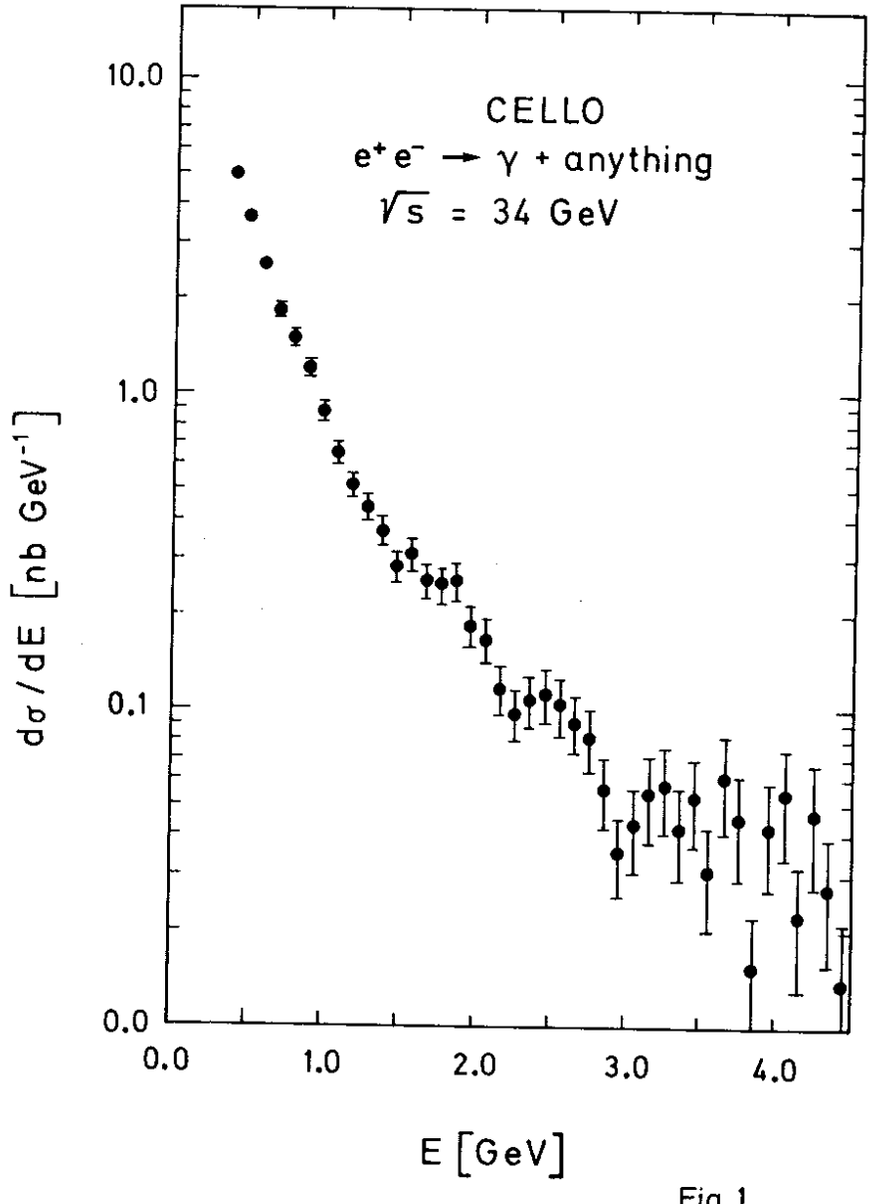

Fig. 1

33816

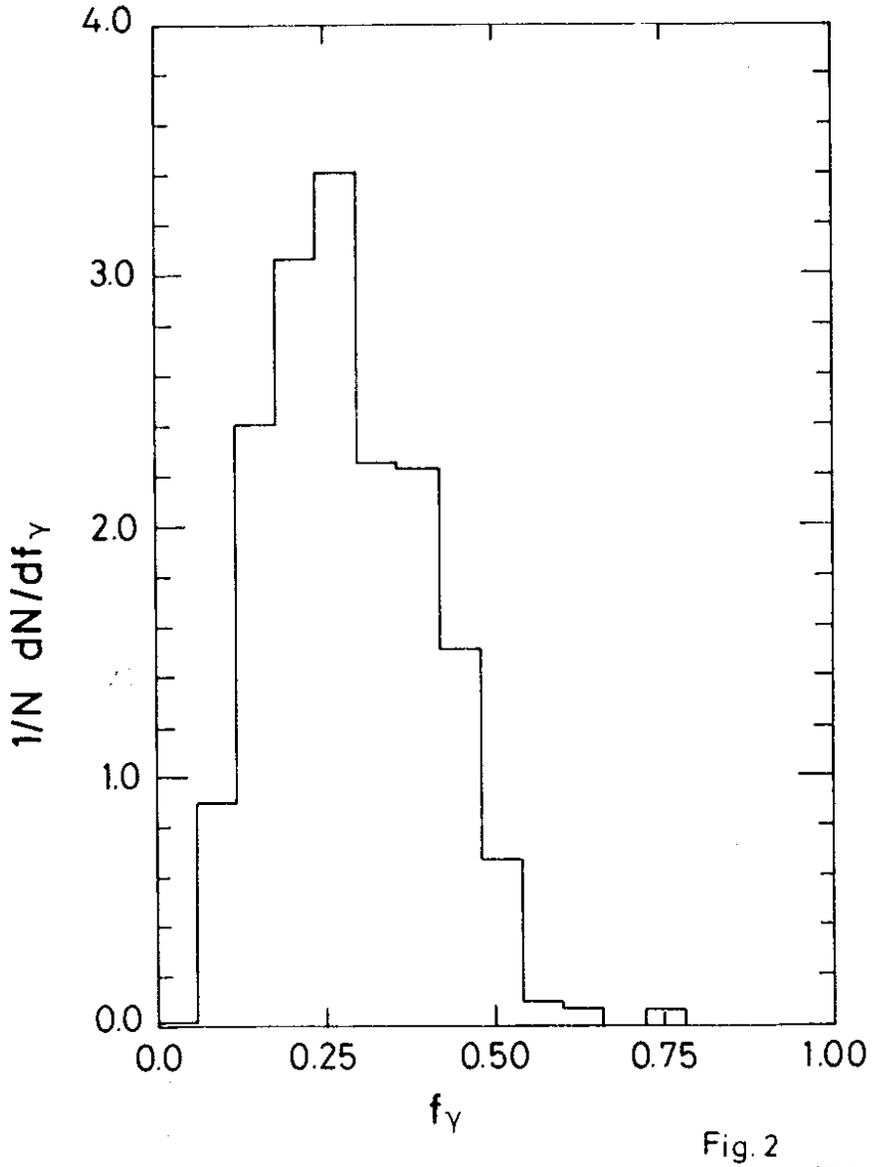

Fig. 2

33817

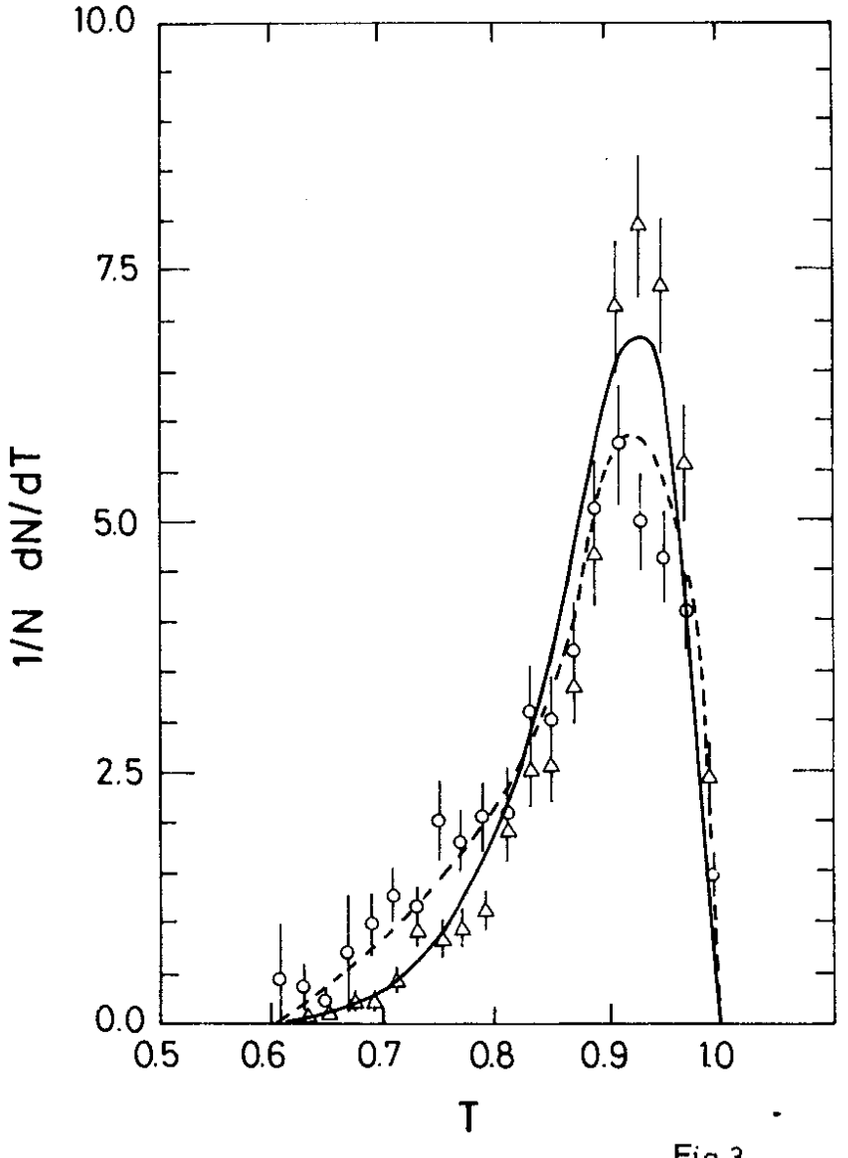

Fig.3

33818

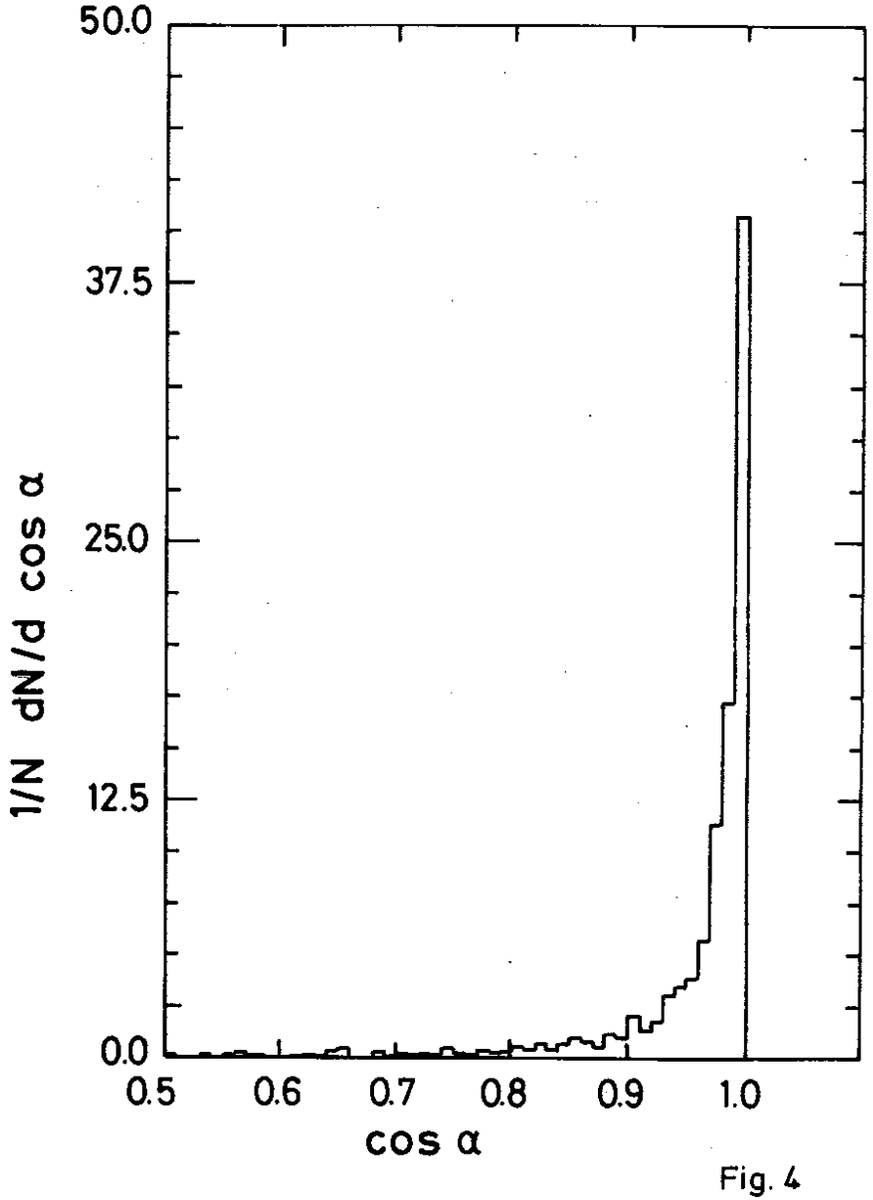

Fig. 4

33819

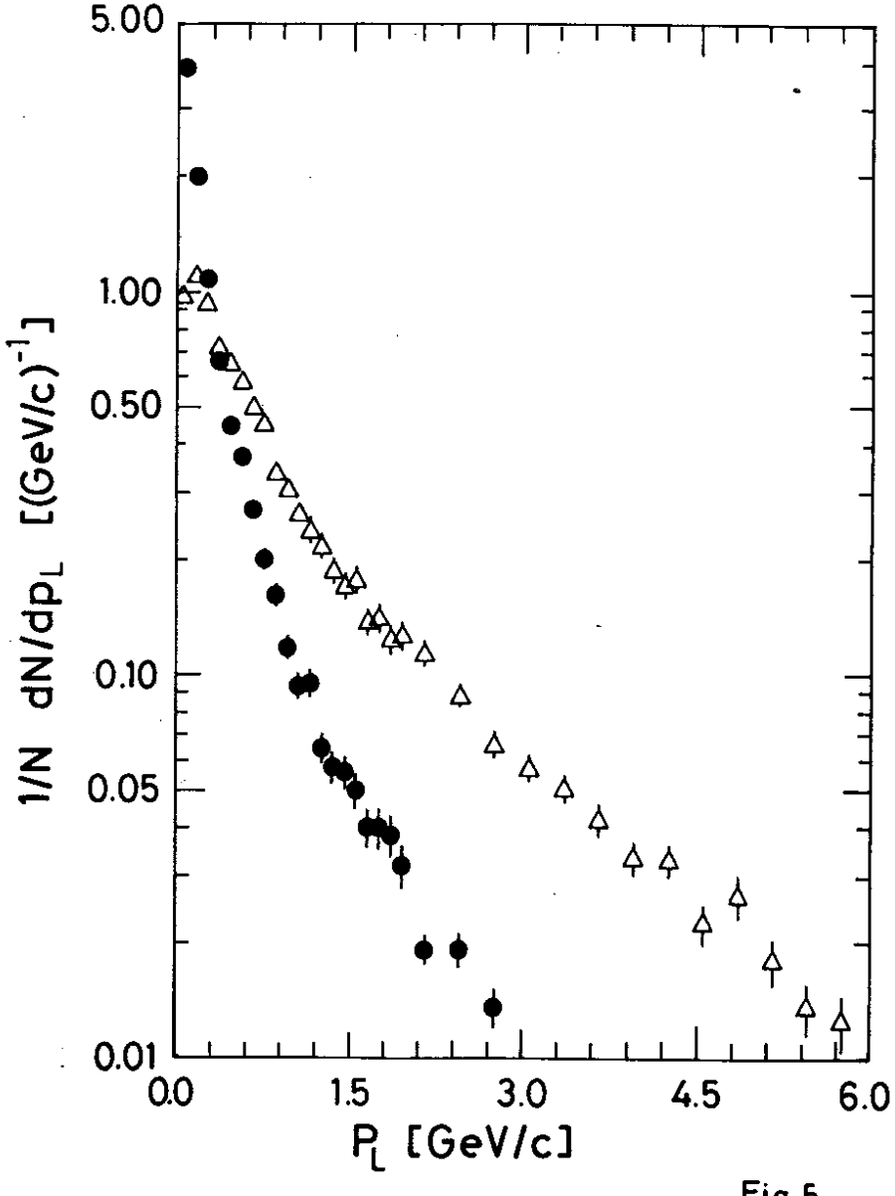

Fig. 5

33820

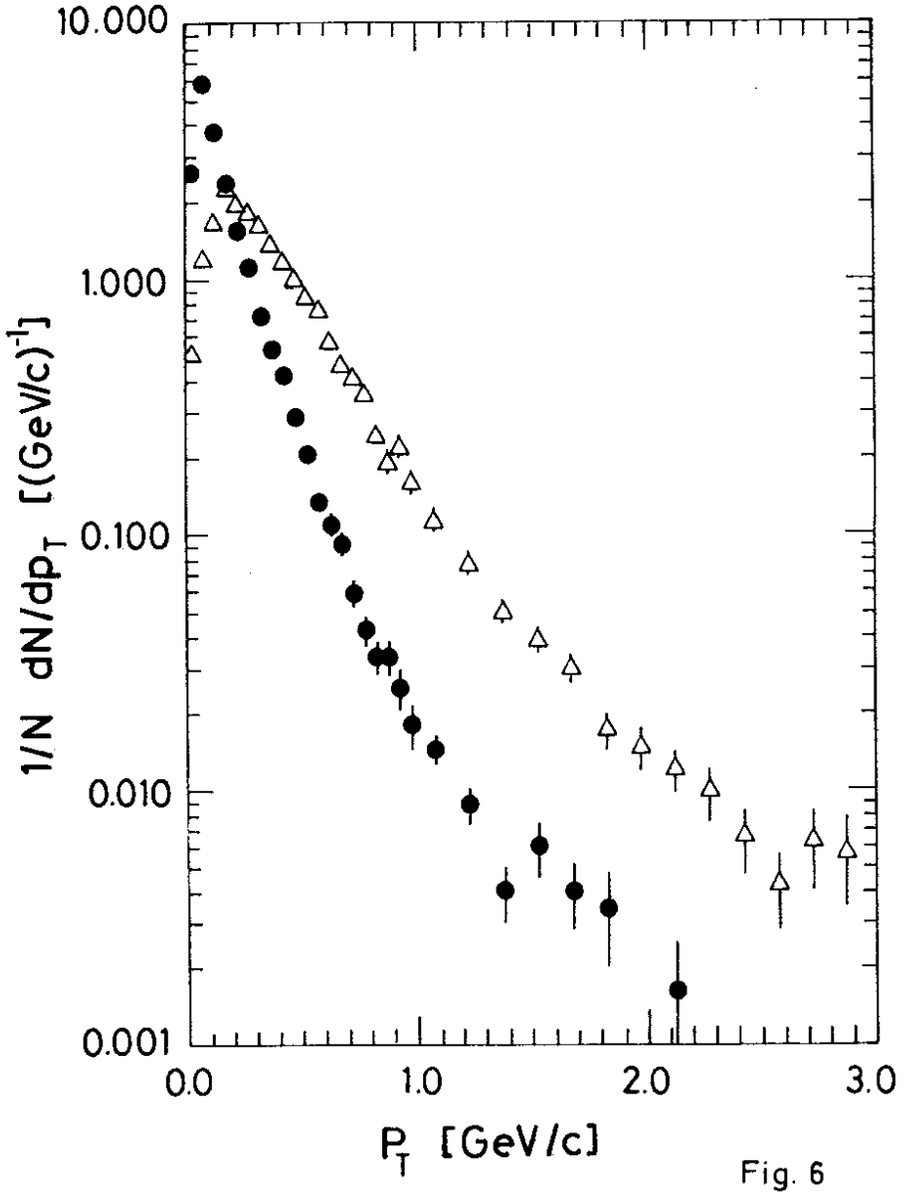

Fig. 6

33821

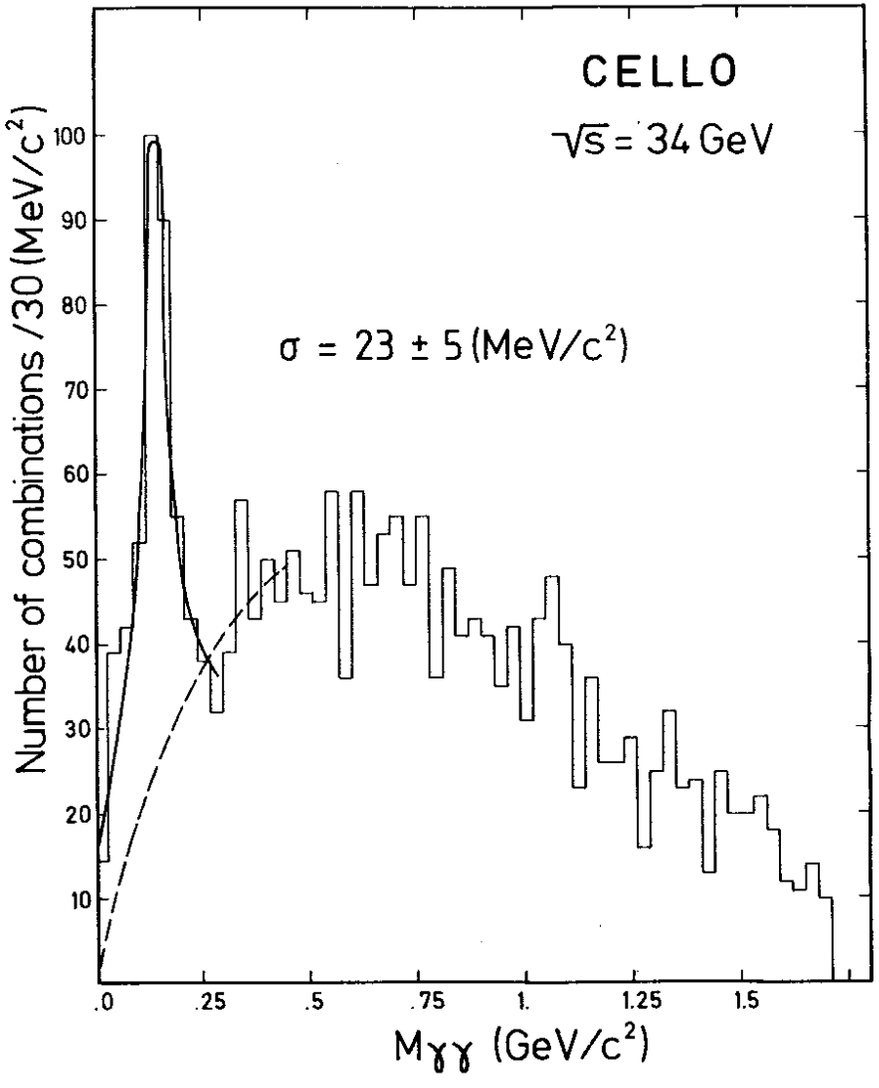

Fig. 7

33822

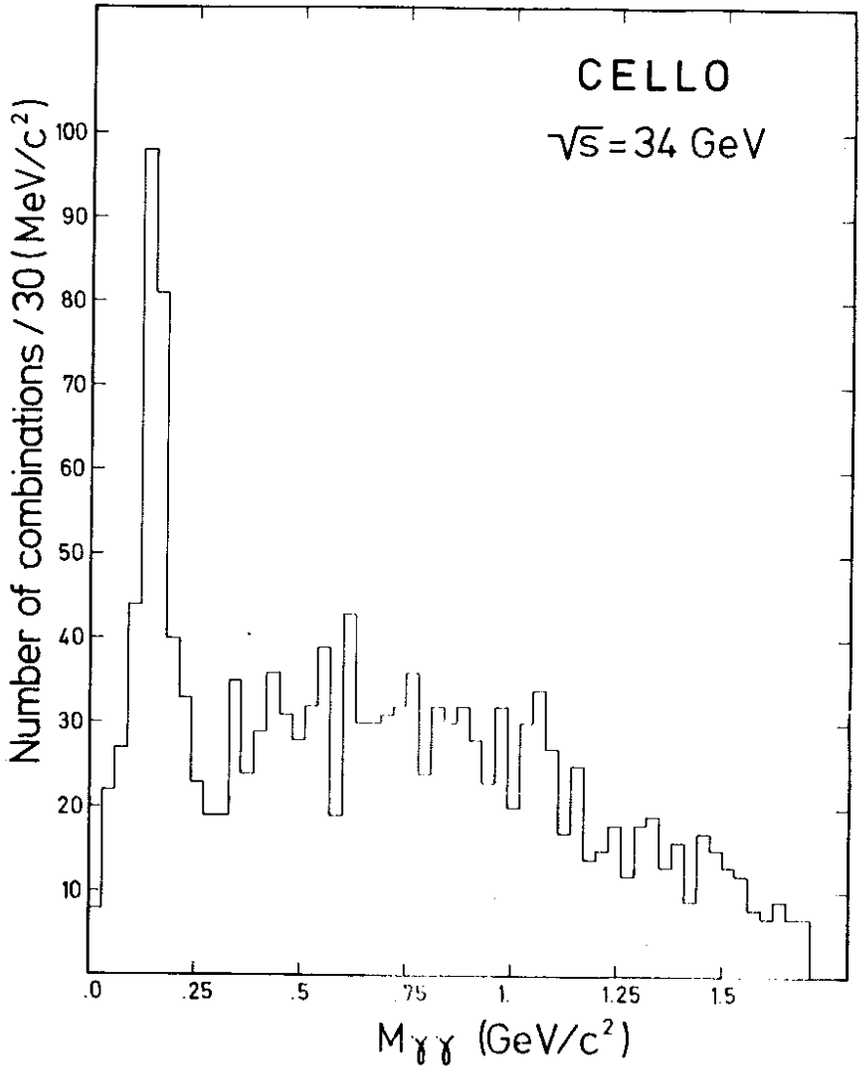

Fig 8

33823

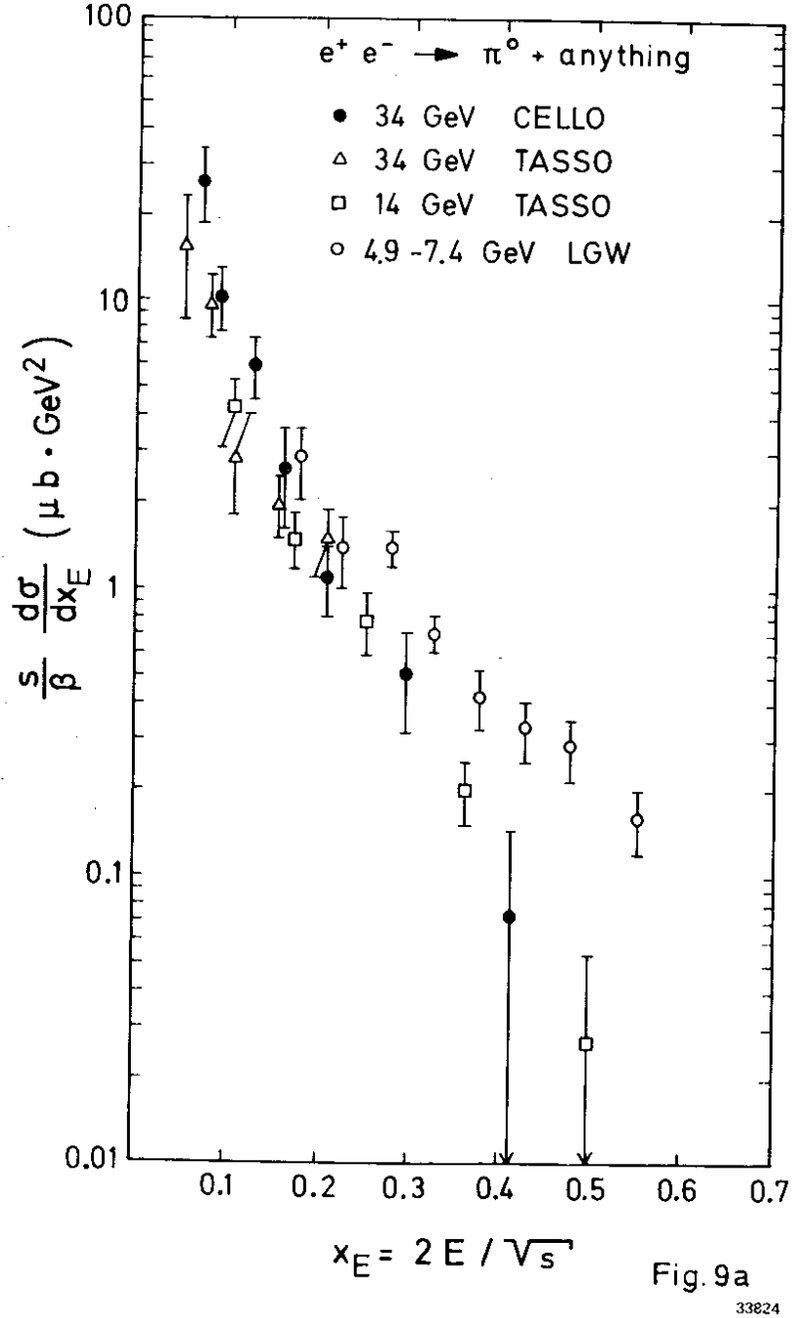

Fig. 9a

33824

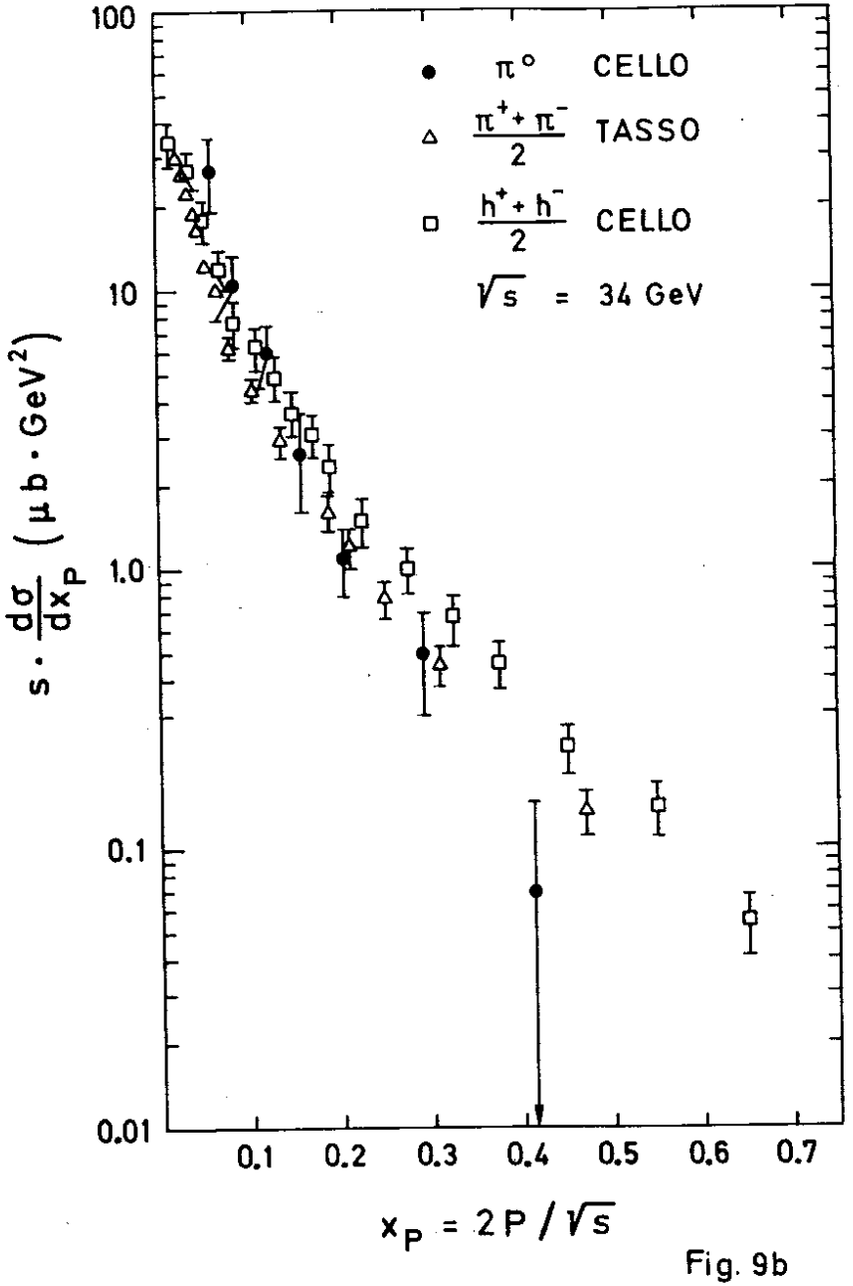
100
10
1.0
0.1
0.01
0.1
0.2
0.3
0.4
0.5
0.6
0.7
π°
CELLO
π⁺+π⁻ / 2
TASSO
h⁺+h⁻ / 2
CELLO
√s = 34 GeV
s · dσ/dx_P (μb · GeV²)
x_P = 2P / √s

Fig. 9b

33825